

Realtime Prediction of Self-Pierce Riveting Joints - Prognosis and Visualization Based on Simulation and Machine Learning

Tobias Falk^{1,a*}, Christian Schwarz^{1,b} and Welf-Guntram Drossel^{1,c}

¹Fraunhofer Institute for Machine Tools and Forming Technology IWU, Nöthnitzer Straße 44, 01187 Dresden, Germany

^atobias.falk@iwu.fraunhofer.de, ^bchristian.schwarz@iwu.fraunhofer.de,
^cwelf-guntram.drossel@iwu.fraunhofer.de

Keywords: Self-Pierce Riveting, Prediction, Machine Learning, Simulation

Abstract. Machine learning is used in many fields nowadays to predict events, be it a pure classification or the prediction of certain values. Thus, these methods are also increasingly used in mechanical joining technology, for example for the prediction of joint strengths, in the classification of defects and rivet head positions or in the prediction of discrete result values such as interlock. This paper further shows how the complete joint contour including the output of stresses, strains and damage can be predicted and visualized in real time for self-piercing riveting with semi-tubular rivet. First, classical sampling is carried out in experiments with steel and aluminum sheets of different types and thicknesses. These are used as a basis for the qualification of the numerical simulations. For this validation experiments and simulations are compared via joint contour and force curves. For the simulations validated in such way several tool variants are carried out in variation calculations for each material-thickness combination. The simulation meshes of the thus generated database are standardized with respect to comparability (same number of nodes) and a data reduction is performed. After testing different approximation approaches, the best possible results are predicted and can be visualized in the developed software demonstrator.

Introduction

An increasingly important topic for stabilizing growth and employment is digitization in production. Mechanical joining technology has a particular role as an interdisciplinary technology and must rely even more strongly on digitalization in the future in order to remain competitive. The integration of machine learning has great potential to implement it in mechanical joining in the production.

A major cost and time factor in the integration of new material combinations is the selection of the most suitable tools. This sampling process has so far mainly been carried out experimentally and requires the expertise and experience of specially qualified employees. In recent years, numerical simulation has been increasingly used as a supporting technology in these sampling processes. However, even these numerical analyses require specialized staff for their setup, calculation and evaluation. Moreover, simulation can only reduce the experimental effort, it cannot replace the sampling as such.

In the latest past, due to increasingly improved and faster computing technology, variant simulations have been carried out in order to be able to make conclusions about the influence of tool geometry parameters (e.g. die depth) on characteristic parameters such as interlock on the base of a large number of numerical calculations [1]. The most recent developments in machine learning were also integrated into the analyses in order to be able to predict result variables [2].

The research mentioned above and other works (prediction of joining forces with neural networks [3], prediction of discrete result values [4, 5]) have been helpful to extend the process understanding of the regarded mechanical joining processes and thus to support the sampling processes. However, these forms of analysis only allow conclusions to be drawn about discrete parameters such as the characteristic value of the undercut. Furthermore, a comprehensive consideration of output values (stress, strain, damage) as in the case of mesh structures in numerical simulations (e.g. maximum principal stress) is not integrated in previous predictions. For this reason, this paper presents a method

using self-pierce riveting as an example, which not only predicts discrete result values when parameters of the sheet properties as well as the die and rivet geometry are entered, but also visualizes a complete joining point contour. Furthermore, the developed software demonstrator offers the possibility to analyze both the sheet metal partners and the rivet with respect to their stresses, strains and damages.

1. State of the Art

1.1. Self-pierce riveting with semi-tubular rivet

Self-pierce riveting with semi-tubular rivet (SPR-ST) is the most used mechanical joining technology for car bodies when using aluminum and steel combinations. This joining method can be sectioned in three steps, shown in **Fig. 1** (left). The first step is characterized by positioning the rivet and the sheets between the punch, blank holder and die (I). When the punch presses the rivet in the punch-sided sheet, the rivet pierces a slug out of the material, which remains inside the cavity (II). The contour of the die forces the rivet to expand and an interlock is created (III). [6]

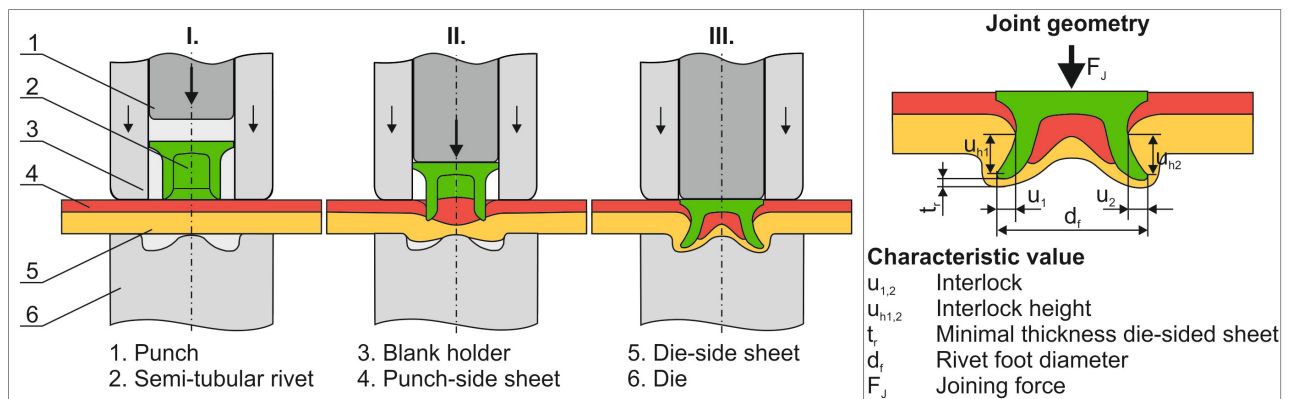


Fig. 1: Process steps of SPR-ST (left); used characteristic values to qualify a SPR-ST joint (right)

The joint geometry at the end of the process has several characteristic values. In this paper the interlock $u_{1,2}$, the interlock height $u_{h1,2}$, the minimal thickness of the die-sided sheet t_r , the rivet foot diameter d_f and the maximum joining force F_j are the important values. The interlock between rivet foot and the die-sided sheet is the essential one, because there is a direct relation to the strength of the joint. Also the minimal thickness of the die-sided sheet is a relevant geometric factor, because if this value is too small, cracking of the joint is possible. [6, 7]

1.2. Machine Learning and mechanical joining

The ability to use machine learning algorithms to predict results in mechanical joining technology has already been used widely. For example, artificial neural networks have been used to predict joint strengths [3], to classify defects in radial clinching [8] and rivet head end position in SPR-ST [9], to predict forces in clinching with divided dies [10], to predict punch force [11] and to generally predict joining ability [12] in SPR-ST. Other algorithms were used, for example, in the prediction of load-bearing behavior of clinch joints (k-nearest neighbors) [13], for the determination of failure values in SPR-ST (XG Boost) [14] or joining point prediction of clinching joints [1], lockbolts [15], self-pierce riveting with solid formable rivet [16] or self-flaring rivet [17] (Kriging, moving least squares, polynomial approaches). These works only allow the prediction of discrete values and not the prediction of a complete joining point contour.

1.3. Principal component analysis (PCA)

Various multivariate statistical methods exist to achieve data compression of higher dimensional data sets. The goal of these methods is to transform the data into a new feature subspace that has a much lower dimensionality than the original space. This type of dimensionality reduction allows the information content to be summarized, making it possible to store and analyze large amounts of data in a simplified and less time-consuming manner [18]. The idea of dimension reduction by principal

component analysis (PCA) consists in a transformation of the higher dimensional original data into a new coordinate system by means of principal axis transformation [19, 20]. In this process, the original data are transformed into a new feature subspace, resulting in a low-dimensional projection matrix [21, 22].

2. Data Base

2.1. Experimental investigations

A large number of experiments have already been carried out in [5], which will be used here. In it, joints for the SPR-ST were investigated in which steel and aluminum sheets were used. The materials and sheet thicknesses for these experiments are summarized in **Table 1**.

Table 1: Investigated materials

Arrangement	Material	$R_m / R_{p0.2}$ [MPa]	Thickness [mm]			
Punch- and die-sided	EN AW-6016 T4	240 / 129	0.8	1.15	1.5	2.0
	EN AW-5182	287 / 144	1.15	1.25	1.5	2.0
	CR210IF	363 / 241	0.8			
	CR3	287 / 144	1.0	1.25	1.5	2.0
	CR330Y590T-DP	627 / 390	1.25	1.5	1.75	2.0
Only punch-sided	CR440Y780T-DP	1035 / 622	1.25			
	CR700Y980T-DP	1022 / 865	1.0			

It should be mentioned that on the die side only steel sheets with $R_m < 650$ MPa were used to avoid extreme rivet deformations. This table also contains the tensile and yield strengths. These were determined in tensile and compression tests for material characterization and a later use in the simulations [23]. For the experimental database, 125 material and thickness combinations were generated with an advanced latin hypercube sampling [24] for a partial factorial investigation. For each joint, the process parameters such as rivet shape and length as well as die design were selected from experience for the best possible joining point characteristics (see **Fig. 2**).

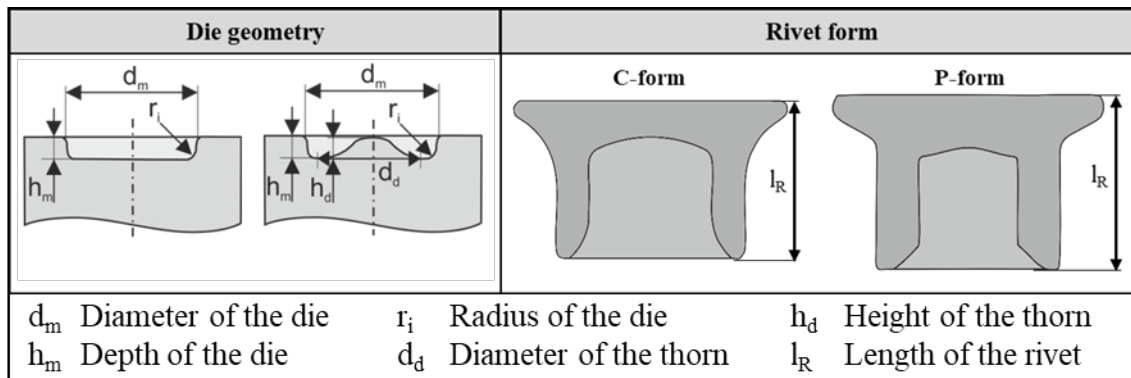


Fig. 2: Applied dies and rivets with their geometric definitions

For the later validation of the simulations, three joining points were examined in cross-section and their force-displacement curves recorded. The fluctuations of the geometric result variables such as interlock and minimal die-side material thickness of the three joining points are on average 20 %. This value is used for later validation to evaluate the predictive capability of the simulations. Of the 125 experiments, 89 designs meet the following minimum requirements:

- Interlock $u_{1,2} \geq 0.15$ mm
- Minimal die-sided material thickness $t_r \geq 0.1$ mm
- Rivet head position $p_h \leq \pm 0.2$ mm
- Rivet foot diameter $d_f \leq 7.8$ mm (Rivet head diameter)
- Crack-free joint

2.2. Numerical simulation and validation

For all experiments, rotationally symmetric 2D simulation models were built up with *Simufact Forming V16*, see **Fig. 3**. The flow curves of the materials for describing the forming behavior in the joining process of the simulation were determined based on tensile and compression tests. The constant parameters of the combined friction model listed therein result from past investigations, sensitivity considerations as well as from adjustments for the best possible match of experiment and simulation over all 125 joints.

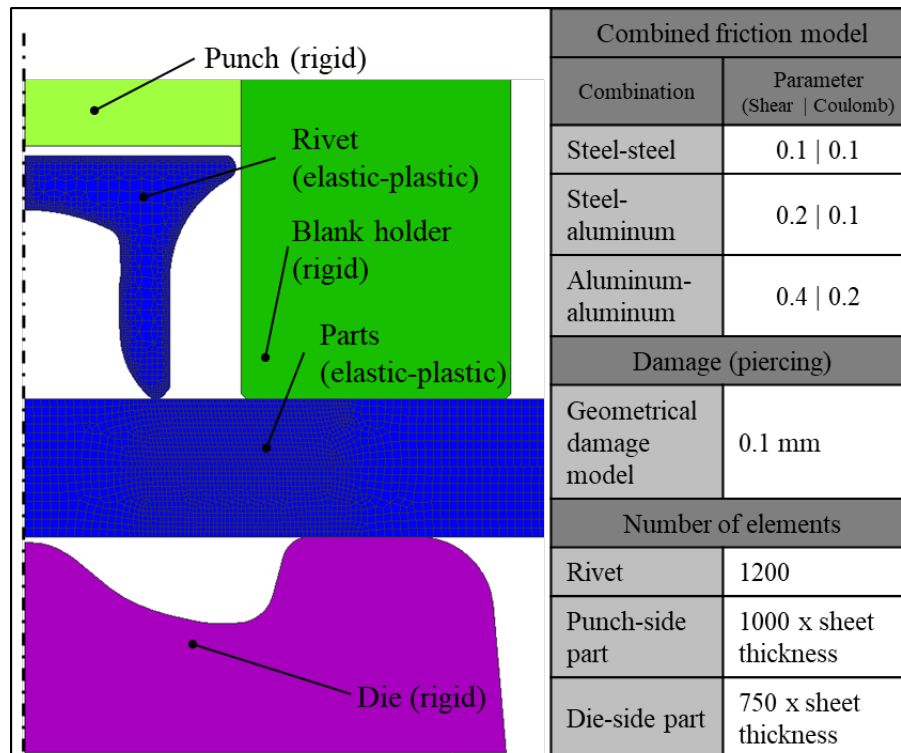


Fig. 3: 2D simulation model and used parameters for the SPR-ST process in Simufact Forming V16

Since numerical sensitivity analyses will be performed based on these validated models in the following, the simulations are created to balance the conflict between high accuracy and short computation time. With the available hardware (workstation with 14 cores), the average simulation time was 13 minutes. **Fig. 4** shows a selection of three joining points. In it, the experiments are compared with the corresponding simulations (red contour) and the resulting output values are shown. It can be seen that for these examples the simulation represents the real experiment sufficiently well. This is the case for 71 compounds, which are included in sensitivity analyses below to generate a larger database.

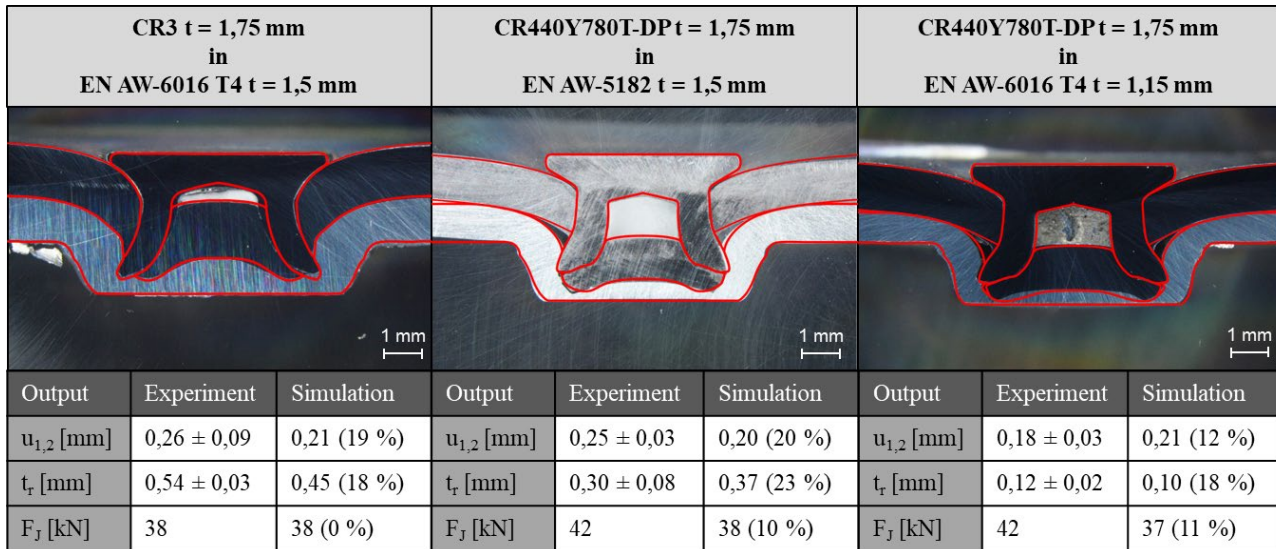


Fig. 4: Validation of the simulation models

2.3. Sensitivity analyses

For each of the 71 simulations, individual sensitivity analyses are performed, each containing 150 parameter sets. Thus, 10650 variant simulations are calculated, in which both process parameters and material properties are varied in relation to the initial value as follows:

- Material properties
 - Sheet thickness: -0.15, -0.1, -0.05, 0, +0.05, +0.1, +0.15 mm
 - Flow curve variation: -20, -15, -10, -5, 0, +5, +10, +15, +20 %
- Rivet properties (compare to Fig. 2)
 - Geometry: C-form, P-form
 - Length (l_R): -0.25, 0, +0.25 mm
- Die geometry (compare to Fig. 2)
 - Die diameter (d_m): -0.5, 0, +0.5 mm
 - Die depth (h_m): -0.25, 0, +0.25 mm
 - Thorn height (h_d): 0.0, 0.5, 1.0, 1.5 mm
 - Thorn width (d_d): 0.0, 2.0, 3.0, 4.0 mm
 - Die edge radius (r_i): 0.1, 0.25, 0.5 mm

Due to the parameter combinations automatically created by ALHS, simulations with tool combinations are generated that are not technologically appropriate or do not produce useful results. Therefore, only the simulation results that are appropriate and target-oriented were used for the integration in the further explanations. Similar to the requirements shown in chapter 3, only the simulations that meet the following less strict criteria are used:

- Interlock $u_{1,2} \geq 0.0$ mm
- Minimal die-sided material thickness $t_r \geq 0.0$ mm
- Rivet head position $p_h \leq \pm 0.5$ mm
- Rivet foot diameter $d_f \leq 8.2$ mm (Rivet head diameter)
- Max. joining force $30 \text{ kN} \leq F_J \leq 85 \text{ kN}$

A total number of 2376 simulations meet these criteria and build the database for the following investigations and the resulting software demonstrator.

3. Data Preparation

3.1. Data standardization

The simulation results are not comparable due to their different parameter designs in terms of number of nodes and mesh structure. However, since this is necessary for the targeted predictions, a standardization must be created for all objects (rivet, slug, punch and die side sheet) of the SPR-ST

and applied to all 2376 simulations. As shown in **Fig. 5** by the example of the rivet, the outer contour points are determined starting from the original simulation mesh (1). Based on this, the outer contour is divided into top and bottom contour, including subdivision (2) and equidistant node points (equal number) are calculated (3). On the resulting connection of outer nodes belonging to each other (top and bottom; 4), the inner node points are again determined equidistantly (5). The number of resulting standardized nodes and elements is thus the same for all simulation results (6) and the resulting mesh structures are comparable.

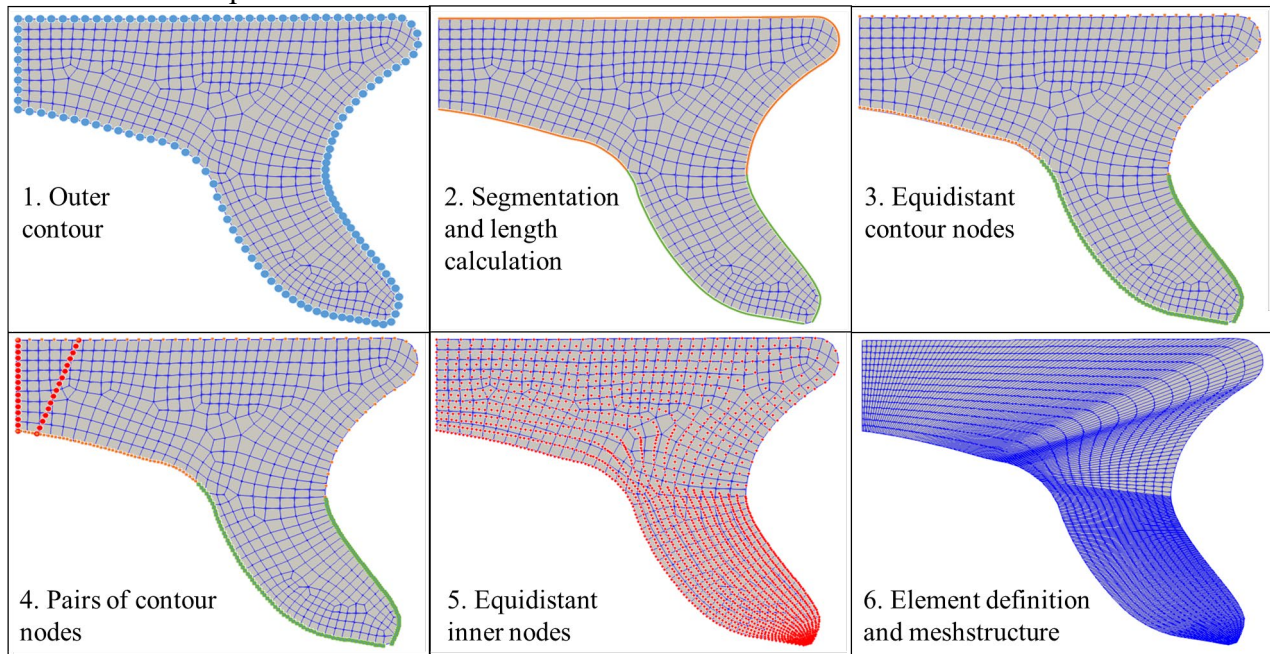


Fig. 5: Standardization of the mesh structure (rivet)

The simulations not only provide the nodal coordinates, but also a lot of additional information for each node, such as deformation, damage (Cockroft & Latham [25]) or maximum principal stress. In order to be able to predict these output values in the later predictions as well, they have to be transferred from the original to the standardized mesh. Since each standardized node (grey, **Fig. 6**) lies within a triangle of three original nodes (black), linear interpolation can be used to first calculate the value of the triangle's base side and then, in the same way, the value of the new, standardized node. This mapping is feasible for all 30 output values (e. g. deformation, damage, maximum principal stress, horizontal displacement) of the simulation software Simufact Forming and is used accordingly in the following prognoses.

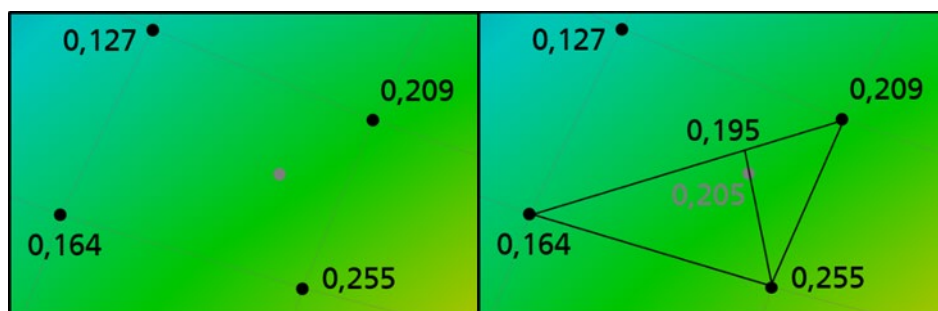


Fig. 6: Mapping of output values from original to standardized node/mesh

The results of the mapping for all joining parts and rivet are shown in **Fig. 7**. There are no obvious differences between the original simulation (left) and the standardized object meshes, neither in the pure geometric form, nor in the mapping of the output size (here: degree of deformation). As mentioned earlier, the total number of standardized nodes is the same for all 2376 simulations and amounts to 4928.

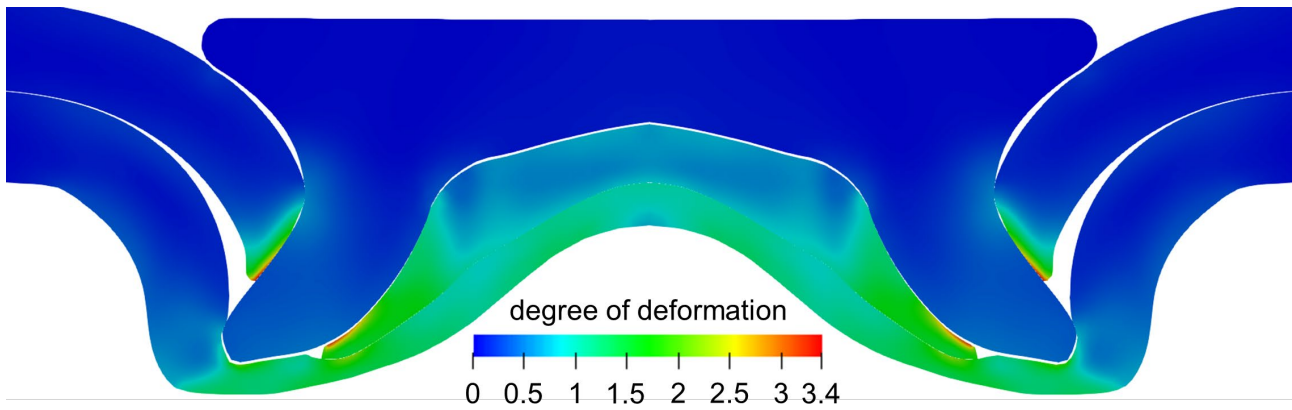


Fig. 7: Comparison the results of the mapping process by the example of degree of deformation: original simulation (left); standardized mesh and mapped results (right)

3.2. Data reduction and prediction modeling

The high number of simulations and nodes is a problem for a fast and precise prediction and cannot be implemented by the prediction models in their current form. Therefore, a data reduction is necessary to enable a fast visualization of the results. At this point, the data are projected using linear principal component analysis (PCA) [19, 20] in a space that has a significantly smaller dimension. The results obtained after the following prediction modeling must therefore be transformed back into the original dimensional space. The PCA is based on the principle of singular value decomposition. With regard to a balanced ratio of computation time and accuracy, 30 principal components are determined for further consideration. Considering that the complexity with this small number of principal components compared to the total number of simulations is close to 1.3 %, the results obtained with this approach are sufficiently good (**Fig. 8**). The difference between the standardized mesh (left) and the mesh generated with the first 30 principal components (right) is hardly visible to the human eye, although a look at the pure numerical values reveals small differences.

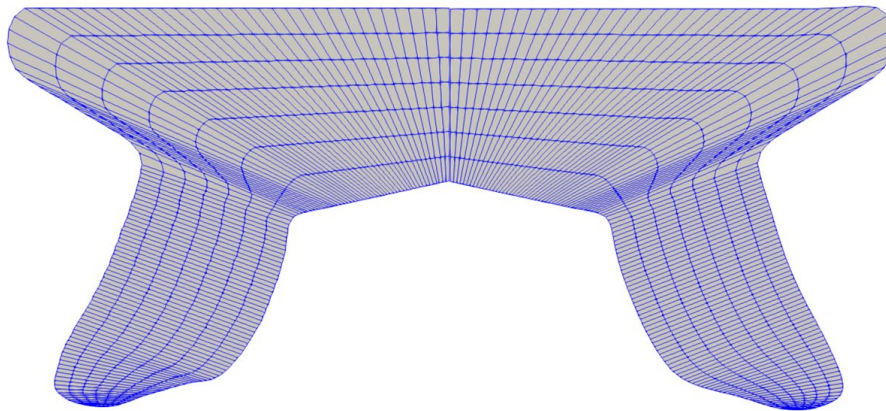


Fig. 8: Comparison the result of nodes/mesh: standardized (left); generated with first 30 linear principal components (right)

Only these 30 principal components are now used for the prediction, and an individual model is determined for each. Due to the fast SPR-ST points to be predicted and visualized, the polynomial approximation approaches [26] shown in **Table 2** are used. Here, for the selection of the best approach, the data is divided into test and training set, and first a model with appropriate approximation coefficients (r_i) is created using the training set. Afterwards, the test data is used to test the accuracy, since for this smaller data set both the original and the predicted values can be compared and the individual approximation approaches and coefficients can be evaluated via the coefficient of determination. By matrix multiplication of these 30 values calculated in this way with a matrix determined in the principal component analysis, the results are transformed back to the original dimension space. This procedure is carried out for the node coordinates in x (horizontal) and z (vertical) direction as well as for all implemented output variables.

Table 2: Implemented approximation approaches

Approximation approach	Mathematical description
Linear basis	$r_0 + \sum_{i=1}^n r_i \cdot x_i$
Linear basis with mixed terms	$r_0 + \sum_{i=1}^n r_i \cdot x_i + \sum_{i,j=1, j>i}^n r_{ij} \cdot x_i \cdot x_j$
Quadratic basis	$r_0 + \sum_{i=1}^n r_i \cdot x_i^2$
Linear and quadratic basis	$r_0 + \sum_{i=1}^n r_i \cdot x_i + \sum_{j=1}^n r_j \cdot x_j^2$
Linear and quadratic basis with mixed terms	$r_0 + \sum_{i=1}^n r_i \cdot x_i + \sum_{i,j=1, i \geq j}^n r_{ij} \cdot x_i \cdot x_j$

4. Software Demonstrator

4.1. Functions and applications

For a user-friendly use of the prediction of the SPR-ST formation, the presented method of standardization, data reduction and prediction modelling has been implemented in a software demonstrator. In this demonstrator (**Fig. 9**), the influence of the 14 input parameters (bottom) on the joining point contour or the node coordinates is displayed (top left). The currently predicted join contour is displayed together with the selected output size (top right). The selected output variable can be displayed as a value for one or more nodes via mouse over or mouse click. In the software demonstrator, the characteristic parameters from **Fig. 1** are calculated and output directly based on the currently predicted joining point contour (middle left).

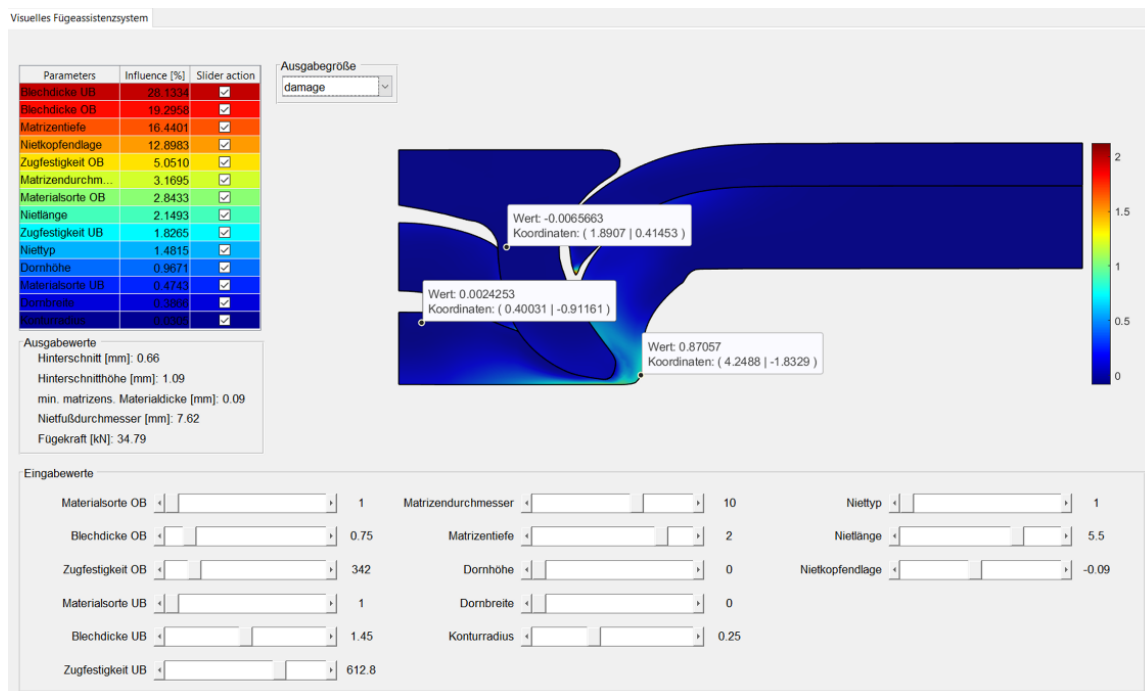


Fig. 9: Software demonstrator – example of a pure steel compound and damage (Cockroft & Latham) as output variable

The 14 input values of the sheet metal properties, die and rivet geometry can be set in an intuitive way using sliders. Immediately after setting the input values, the predicted joint is displayed in real time, including the selected output variable and the measurement of the characteristic values. If a

different output size is selected, the clicked nodes will remain, only the value changes according to the new output variable.

4.2. Verification

In order to evaluate the quality of the predictions, comparisons of simulated and predicted joining point results for different sheet pairings are shown in **Fig. 10**. In view of the fast result presentation (less than one second with the software demonstrator compared to 10 to 15 minutes for the pure simulation calculation), the small differences are acceptable. Thus, the developed software demonstrator can be used as an assistant tool for the sampling process to speed it up efficiently.

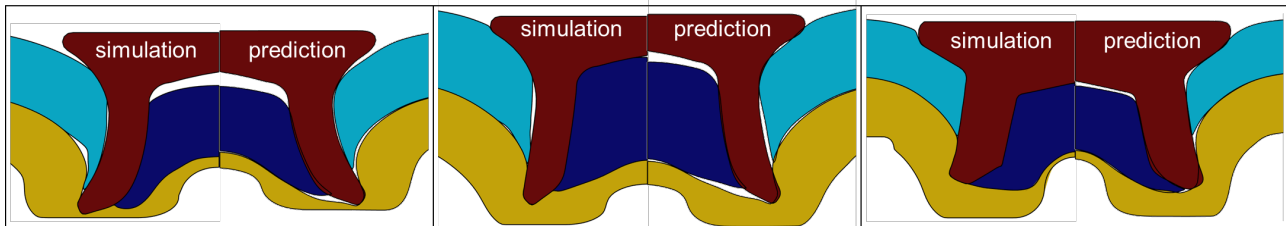


Fig. 10: Comparison of simulation and prediction for different SPR-ST joint contours: steel-aluminum (left); aluminum-aluminum (middle); steel-steel (right).

Summary

Based on more than 2300 simulations of the SPR-ST process, a method has been developed that enables the real-time prediction of previously not simulated sheet metal pairings, tool and rivet geometries using mesh standardization, dimensional reduction and prediction modeling. For the visualization of these results, an intuitive software demonstrator has been programmed, which allows non-specialist users to virtually simulate SPR-ST joints. This demonstrator can thus support the experimental sampling process and make it more efficient if, for example, the effects of changed die parameters on the joining point are displayed while the sheet properties remain unchanged. In principle, further simulation calculations can be integrated into the existing system. The basic features of the developed method can also be transferred to other mechanical joining processes.

Acknowledgement

The presented results are part of the research project “Visual joining assistance system” (20630BR) of the European Research Association for Sheet Metal Working (EFB) funded by the program for “Industrial Collective Research” (IGF) of the Federal Ministry of Economic Affairs and Climate Action (BMWK) and the German Federation of Industrial Research Association (AiF).

References

- [1] Drossel, W.-G.; et al: Unerring Planning of Clinching Processes through the Use of Mathematical Methods, KEM 611–612, 1437–1444, 2014.
- [2] Jäckel, M.; et al: Gathering of Process Data through Numerical Simulation for the Application of Machine Learning Prognosis Algorithms. Procedia Manufacturing, 47, 608-614, 2020.
- [3] Thoms, V.; Kalich J.: Prozessvorhersage beim Stanznieten mit neuronalen Netzen, EFB-Forschungsbericht, Nr. 179, Hannover, 2002.
- [4] Tassler, T.; et al: Verbesserung der Vorhersagegenauigkeit von Metamodellen. Forschung im Ingenieurwesen 81-4, 373 – 382, 2017.
- [5] Jäckel, M.; et al: Gathering of Process Data through Numerical Simulation for the Application of Machine Learning Prognosis Algorithms, Procedia Manufacturing 47: 608-614, 2020.
- [6] Hahn, O.; Klemens, U.: Fügen durch Umformen, Nieten und Durchsetzfügen-Innovative Verbindungsverfahren für die Praxis, Studiengesellschaft Stahlanwendung, 1996.

-
- [7] DVS/EFB 3410: Merkblatt Stanznieten-Überblick, DVS-Verlag, Düsseldorf, 2018.
- [8] Breckweg, A.: Automatisiertes und prozessüberwachtes Radialclinchen höher-fester Blechwerkstoffe. Dissertation. Stuttgart 2006.
- [9] Schromm, T.; Diwald, F.; Grosse, C.: An attempt to detect anomalies in car body parts using machine learning algorithms, IEEE Transactions on Systems, Man and Cybernetics 9-1, 62–66, 2019.
- [10] Lambiasi, F.; Di Ilio, A.: Optimization of the Clinching Tools by Means of Integrated FE Modeling and Artificial Intelligence Techniques. Procedia CIRP 12, 163–168, 2013.
- [11] Oh, S.; et al: Deep-Learning-Based Predictive Architectures for Self-Piercing Riveting Process, IEEE Access 8, 116254–116267, 2020.
- [12] Karathanasopoulos, N.; Pandya, K. S.; Mohr, D.: Self-piercing riveting process: Prediction of joint characteristics through finite element and neural network modeling. Journal of Advanced Joining Processes 3, 100040, 2021.
- [13] Tan, Y.: Vorhersage des Tragverhaltens von Clinchverbindungen unter quasi-statischer Scherzugbelastung mittels eines neuronalen Netzes, Universität Paderborn Dissertation, 2003.
- [14] Lin, J.; et al: Prediction of cross-tension strength of self-piercing riveted joints using finite element simulation and XGBoost algorithm, Chinese Journal of Mechanical Engineering 34.1, 2021.
- [15] Wanner, M.-C.; et al: Numerische und experimentelle Untersuchung von Setzprozess-unregelmäßigkeiten bei Schließringbolzensystemen, Ergebnisse eines Forschungsvorhabens der industriellen Gemeinschaftsforschung (IGF), EFB-Forschungsbericht 426, Hannover 2015.
- [16] Grimm, T.; et al: Technologies for the mechanical joining of aluminum die castings, AIP Conference Proceedings, Vol. 2113, No. 1, AIP Publishing LLC, 2019.
- [17] Kraus, C.; et al: Development of a new self-flaring rivet geometry using finite element method and design of experiments, Procedia Manufacturing 47, p. 383-388, 2020.
- [18] Raschka, S.: Python machine learning – Unlock deeper insights into machine learning with this vital guide to cutting-edge predictive analytics, Packt publishing ltd, 2015.
- [19] Pearson, K.: On lines and planes of closest fit to systems of points in space, Philosophical Magazin 2, 559-572, 1901.
- [20] Hotelling, H.: Analysis of a complex of statistical variables into principal components, Journal of Educational Psychology 24 6, p. 417–441, 1933.
- [21] Jolliffe, I.: Principal component analysis, Encyclopedia of statistics in behavioral science, 2005.
- [22] Jackson, J. E.: Principal Components and Factor Analysis: Part I—Principal Components. Journal of Quality Technology 12-4, p. 201–213, 1980.
- [23] Jäckel, M.; et al: Process-oriented Flow Curve Determination at Mechanical Joining, Procedia Manufacturing, Vol.47, 368-374, 2020.
- [24] McKay, M. D.; Beckman, R. J.; Conover, W. J.: A Comparison of Three Methods for Selecting Values of Input Variables in the Analysis of Output from a Computer Code, Technometrics 21 2, p. 239, 1979.
- [25] Cockroft, M. G.; Latham, D. J.: Ductility and Workability of Metals, Journal of the Institute of Metals 96, 33-39, 1968.
- [26] Clarkson, J. A., & Erdős, P.: Approximation by polynomials, Duke Mathematical Journal, 10(1), 5-11, 1943.